JACS
JOURNAL OF THE AMERICAN CHEMICAL SOCIETY
ARTICLE
pubs.acs.org/JACS

# Spatial Correlations of Density and Structural Fluctuations in Liquid Water: A Comparative Simulation Study

Felix Sedlmeier,[†] Dominik Horinek,[†,‡] and Roland R. Netz[*,†]

[†]Physik Department, Technische Universität München, 85748 Garching, Germany
[‡]Institut für Physikalische und Theoretische Chemie, Universität Regensburg, 93040 Regensburg, Germany

S Supporting Information

**ABSTRACT:** We use large-scale classical simulations employing different force fields to study spatial correlations between local density and structural order for water in the liquid temperature range. All force fields investigated reproduce the main features of the experimental SAXS structure factor $S(q)$, including the minimum at small $q$, and the recent TIP4P/2005 parametrization yields almost quantitative agreement. As local structural order parameters we consider the tetrahedrality and the number of hydrogen bonds and calculate all pure and mixed spatial two-point correlation functions. Except for the density−density correlation function, there are only weak features present in all other correlation functions, showing that the tendency to form structural clusters is much weaker than the well-known tendency of water to form density clusters (i.e., spatially correlated regions where the density deviates from the mean). In particular, there are only small spatial correlations between local density and structural fluctuations, suggesting that features in density−density correlations (such as measured by the structure factor) are not straightforwardly related to spatial correlations of structure in liquid water.

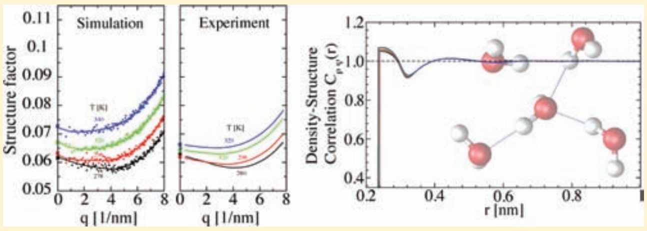

## INTRODUCTION

As is commonly said, water is the most essential substance in nature. At the same time, water is surprisingly difficult to understand, partly due to anomalous behavior in almost all thermodynamic observables.[1] The best-known example is certainly the anomaly in the water density, which shows a maximum at 4 °C, at which temperature the thermal expansion coefficient $\alpha_P = 1/V(\partial V/\partial T)_P$ changes sign. But also other thermodynamic properties, like the isothermal compressibility $\kappa_T = -1/V(\partial V/\partial P)_T$ and the isobaric heat capacity $C_P = (\partial H/\partial T)_P$, exhibit anomalies: at atmospheric pressure, $\kappa_T$ has a minimum at 46 °C and $C_P$ has a minimum at 35 °C.[2−5] This stands in marked contrast to the behavior of simple liquids, whose thermodynamic properties vary monotonously with temperature.

Despite intense efforts for many years, there is still no complete and simple explanation for these anomalies. Several hypotheses have been proposed,[6−8] among which the liquid−liquid critical point (LLCP) scenario has received much support in the recent literature. According to the LLCP scenario, water possesses a metastable critical point at very low temperatures which marks the end point of a first-order phase transition between a high-density (HDL) and a low-density (LDL) liquid phase. The LDL phase is associated with tetrahedral-like local structure, while the HDL phase corresponds to a local structure with distorted hydrogen bonds.[9,10] The anomalous temperature dependence of the thermodynamic response functions then follows naturally, since they are expected to diverge at the transition line or exhibit maxima or minima at the continuation of the transition line into the one-phase region.[9] However, conclusive experimental evidence for this scenario is still missing, and the connection between anomalous water properties and the existence of low-temperature singularities is controversially discussed.[9,11]

Recently, it has been suggested that remnants of these phases persist even at higher temperatures and that extended clusters of HDL and LDL are present at ambient conditions.[12] These conclusions were partly based on the well-known experimental observation that the structure factor $S(q)$, obtained from SAXS or neutron scattering, shows an enhancement at very low wave vectors $q$.[13−16] In conjunction with X-ray adsorption, Raman, and emission spectroscopy, it was argued that the density fluctuations manifest in $S(q)$ originate from concentration fluctuations of two structurally distinct liquid species differing in density.[12] From an Ornstein−Zernike (OZ) analysis of the scattering data, the typical size of these clusters was estimated to be on the order of ~1 nm. It was also stated that standard three-point water models such as SPC/E are not able to reproduce the minimum in the structure factor,[12] from which it was concluded that the local water structure is ill-reproduced by current classical simulation models for water.

The relationship between the density and structure of water has been much discussed in recent literature,[16−19] partly because this relation is crucial for understanding the water density anomaly. Using an analysis of structural water clusters in SPC/E water simulations, Errington et al.[17] have found a decrease in the density of water clusters with both increasing tetrahedrality

**Received:** July 20, 2010
**Published:** January 14, 2011

and increasing cluster size at temperatures of $T = 220$ and 240 K. This suggests that the formation of tetrahedrally ordered low-density water is cooperative. Moore and Molinero[18] used the monatomic mW[20] water model for an extensive study of the water structure in the temperature range from 100 to 350 K. They found an increase in the average tetrahedrality and the fraction and cluster size of four-coordinated molecules upon cooling. However, they did not observe a low-$q$ enhancement of the structure factor, which they attributed to the lack of density difference between differently coordinated water molecules in the mW model.[18] Only when they restricted the calculation of the structure factor to four-coordinated water molecules did they see an increase for low $q$, from which they inferred correlation lengths that grow with decreasing temperature, using an OZ analysis. Matsumoto[19] showed that the change in the average composition of differently coordinated water molecules upon cooling is not correlated with the mean density of the liquid. He could accurately explain the temperature dependence of the density by taking into account the interplay of the average bond length, which decreases upon cooling and therefore tends to increase the density, and the distortion of the tetrahedral bonding network, which decreases upon cooling and thereby decreases the density. Very recently, Soper et al.[21] and Clark et al.[16] argued that an enhancement in the low-$q$ region of the structure factor is consistent with normal particle number fluctuations and does not necessarily indicate the presence of two structural water species with different densities. Furthermore, it was shown that the OZ analysis applied in ref 12 to infer a spatial scale of regions with correlated densities is not very meaningful far away from a critical point. Clark et al.[16] very convincingly demonstrated the absence of pronounced density inhomogeneities on length scales ranging from 0.6 to 6 nm based on the unimodality of density histograms obtained by simulations of TIP4P-Ew water,[16] thus casting additional doubt on the interpretation of $S(q)$ data as a sign of the coexistence of two different local structural motifs in liquid water.[12]

While the relation between spatially averaged structural properties and the mean density of water seems well understood, the question of the existence and spatial size of structurally correlated regions in liquid water is less clear. In particular, the discussion in ref 12 raised the question to what degree the spatial extent of density correlations (as directly inferred from SAXS experiments via the structure factor) is related to the size of structurally correlated water patches (which can only indirectly be inferred from experiments). Instead of using clustering algorithms to define the size of regions with high structural order,[17−19] we determine spatial two-point correlation functions involving the local density and different local structural order parameters, namely the tetrahedrality order parameter,[22−24] $\psi$, and the number of hydrogen bonds a water molecule forms with its neighbors, $n_{\mathrm{HB}}$. By using the exact same mathematical form for assessing the presence of spatial correlations of density and structural fluctuations, we are able to make a simple and meaningful comparison between density−density correlations (expressed in terms of the well-known radial distribution function) and density−structure and structure−structure correlations. Except for the density−density correlation function, we find only weak correlations that decay to zero within a few angstroms. This means that although water is a highly structured fluid, the structure shows only weak spatial correlation and that the coupling between density and structural fluctuations is also quite weak when compared with the degree to which density−density correlations are present.

In order to check how robust the simulated structure factor is with respect to force field modifications, we compare the SPC/E,[25] TIP4P/2005,[26] and TIP5P[27] water models. The SPC/E, TIP4P/2005, and TIP5P water models all have a rigid geometry with fixed point charges and a varying number of interaction sites. All of them have two positively charged hydrogen atoms and an oxygen atom on which the Lennard-Jones interaction is centered. They differ mainly in the placement of the negative charge. In the SPC/E water model the negative charge is placed on the oxygen atom, while in the TIP4P/2005 water model the negative charge is placed on an additional virtual site on the bisector of the HOH angle. In the TIP5P model the negative charge is placed on two virtual sites located on the edges of a slightly distorted tetrahedron, formed by the two hydrogen atoms and the two virtual sites. The SPC/E water model has a density maximum at $T = 235$ K[28] and a minimum in $\kappa_T$ around $T = 270$ K[29] and thus differs considerably from the experimental values. It exhibits the LDA and HDA phases in the amorphous state,[30,31] and it has been suggested that it has a LLCP.[32] The TIP5P water model has been parametrized to yield the correct position of the density maximum at $T = 277$ K[27] using a reaction field method to account for electrostatic periodic boundary conditions. Note that in combination with the Particle Mesh Ewald summation method,[33,34] as used in this paper, the density maximum is shifted slightly to $T = 284$ K.[35] It has been shown that the TIP5P water model shows a LLCP[31,36] and that its isobaric heat capacity shows a sharp increase for decreasing temperature,[31] in accordance with the experimental data. The isothermal compressibility of the TIP5P water model does not show a minimum within the range studied so far.[29] The TIP4P/2005 model is a recent reparameterization of the widely used TIP4P[37] water model. It excellently reproduces the temperature dependence of the density as well as the isothermal compressibility at atmospheric pressure, exhibiting a density maximum at $T = 278$ K[26] and a minimum in $\kappa_T$ at $T = 310$ K.[29] The TIP4P model has a LLCP,[31] so it is likely that the TIP4P/2005 model has a LLCP, too. We find that all three water models exhibit an enhancement of the structure factor for low $q$, which is pronounced for the TIP5P and TIP4P/2005 water models and still perceptible for the SPC/E water model. The TIP4P/2005 model almost quantitatively accounts for the experimental structure factor in the low-$q$ region, while the TIP5P and SPC/E models show various degrees of deviation. Together with the results of Clark et al.,[16] who found a minimum of $S(q)$ using the TIP4P-Ew water model in very good agreement with experiment, this shows that the scattering enhancement at low $q$ is a quite robust feature of simple classical water models and does not point to any subtle structural property of water that is missed by these models. Clearly, the accurate determination of the low-$q$ region of the structure factor is a challenging task in simulations, since in a finite system the minimal accessible wave vector and the resolution in reciprocal space are inversely proportional to the system size. Therefore, large systems are necessary, leading to high computational costs. Furthermore, the method to extract the structure factor from simulation trajectories has to be chosen with care, since finite size artifacts can otherwise obscure the results.[38] Clark et al.[16] managed to reduce Fourier truncation ripples by performing simulations in the grand canonical ensemble. We compare several methods to extract the structure factor from simulations in the canonical ensemble that yield a consistent picture of the low-$q$ region of the structure factor.

## METHODS

We use molecular dynamics (MD) simulations to obtain information about density and structural correlations of water in the liquid temperature range (for simulation details see Supporting Information).

**Structure Factor.** On the two-point level, the density correlations of a fluid are characterized by the pair distribution function,

$$g(\vec{r},\vec{r}\,') = \frac{\langle \rho^{(2)}(\vec{r},\vec{r}\,')\rangle}{\langle \rho(\vec{r})\rangle\langle \rho(\vec{r}\,')\rangle} \tag{1}$$

where $\rho^{(2)}(\vec{r},\vec{r}\,') = \sum_{i,j=1;i\neq j}^{N}\delta(\vec{r}-\vec{r}_i)\delta(\vec{r}\,'-\vec{r}_j)$ and $\rho(\vec{r}) = \sum_{i=1}^{N}\delta(\vec{r}-\vec{r}_i)$ are the two- and one-particle density operators, $N$ is the number of particles, and $\vec{r}_i$ is the position of the $i$th particle. For a homogeneous and isotropic system, $g(r) = g(\vec{r},\vec{r}\,')$ is a function of the distance $r = |\vec{r} - \vec{r}\,'|$ only and is called the radial distribution function (RDF). The RDF can be extracted straightforwardly from a MD simulation by generating a histogram of interparticle distances and appropriate normalization. Scattering experiments measure the structure factor $S(q)$, defined as

$$S(\vec{q}) = \left\langle \frac{1}{N}\sum_{i,j=1}^{N} \mathrm{e}^{-\mathrm{i}\vec{q}\cdot(\vec{r}_i-\vec{r}_j)} \right\rangle \tag{2}$$

For a homogeneous and isotropic system, it is a function of $q = |\vec{q}|$ only and related to the RDF by a Fourier transformation,[39]

$$S(q) = 1 + 4\pi\rho\int_0^\infty \mathrm{d}r r\frac{\sin(qr)}{q}(g(r)-1) \tag{3}$$

where $\rho = \langle\rho(\vec{r})\rangle = N/V$ is the number density of the fluid. Equation 3 constitutes the first of the two methods used to calculate the structure factor in this paper (FT method) and is based on the RDFs obtained from MD simulations. Note that we take only the oxygen atoms of the water molecules into account, thereby assuming that the electron density of the water molecule is approximately spherical and centered around the oxygen atom.[40] Due to the periodic boundary conditions and the minimum image convention used in the MD simulation, the RDF can only be obtained up to a radius $r_{\max} = L/2$, where $L$ is the length of the periodic box. Therefore, the upper boundary in the integral in eq 3 has to be replaced by $r_{\max}$, which leads to pronounced "cutoff ripples", especially for low wave vectors $q$,[38] and effectively restricts the use of eq 3 to the range $q > q_{\min}^{\mathrm{FT}} = 2\pi/r_{\max}$. The cubic simulation box we use in this study has a size of $L \approx 10$ nm, and thus $q_{\min}^{\mathrm{FT}} \approx 1.2$ nm$^{-1}$. Due to the $r$ factor in the integrand of eq 3, these cutoff artifacts are increased even by minute numerical errors in the RDF at larger radii, which might be introduced, for example, by round-off errors. To enforce that the RDFs correctly converge to 1 for large $r$, we calculate the average of the RDF over the interval 3 nm < $r$ < 5 nm and divide the RDF by that average. Typically, the deviations of the average from 1 before the normalization are on the order of $10^{-5}$.

Since the aforementioned subtleties in the application of eq 3 to calculate the structure factor prohibit a clear interpretation of $S(q)$, especially in the low-$q$ limit we are interested in, we also calculate the structure factor directly from the simulation trajectories by applying the definition in eq 2. One can rewrite eq 2 in the following way,

$$S(\vec{q}) = \left\langle \frac{1}{N}\Big[\sum_{i=1}^{N}\sin(\vec{q}\cdot\vec{r}_i)\Big]^2 \right\rangle + \left\langle \frac{1}{N}\Big[\sum_{i=1}^{N}\cos(\vec{q}\cdot\vec{r}_i)\Big]^2 \right\rangle \tag{4}$$

which is more convenient for evaluation from a simulation trajectory, since it contains only single sums. Equation 4 constitutes the second method used to calculate the structure factor in this paper (D method). Due to the finite size of our simulation system, $S(\vec{q})$ can only be evaluated for wave vectors $\vec{q} = (n_x,n_y,n_z)2\pi/L$, where the $n_i$ are integers and $L$ is the length of the simulation box, which in our simulations is cubic. The minimum wave vector that can be sampled is therefore given by $q_{\min}^{\mathrm{D}} = 2\pi/L$ and thus smaller by a factor of 2 compared to that obtained by the FT method, leading to $q_{\min}^{\mathrm{D}} \approx 0.6$ nm$^{-1}$ for the box size used in this study.

**Table 1. Densities, Compressibilities, and Mean Structural Order Parameters for the Studied Water Models Obtained from MD Simulations at a Pressure of $P$ = 1 bar**

| water model | $T$ (K) | $\rho$ (kg/L) | $\kappa_T$ ($10^{-11}$ Pa$^{-1}$) | $S(q{=}0)$ | $\langle\psi\rangle$ | $\langle n_{\mathrm{HB}}\rangle$ |
|---|---|---|---|---|---|---|
| SPC/E | 278 | 1.008 | 44.32 | 0.057 | 0.661 | 3.69 |
| SPC/E | 298 | 0.999 | 45.50 | 0.063 | 0.635 | 3.61 |
| SPC/E | 320 | 0.987 | 48.23 | 0.070 | 0.609 | 3.51 |
| SPC/E | 340 | 0.973 | 51.53 | 0.079 | 0.588 | 3.41 |
| TIP5P | 278 | 0.986 | 52.62 | 0.067 | 0.713 | 3.51 |
| TIP5P | 298 | 0.983 | 55.30 | 0.075 | 0.661 | 3.34 |
| TIP5P | 320 | 0.969 | 60.80 | 0.087 | 0.615 | 3.16 |
| TIP5P | 340 | 0.949 | 69.47 | 0.103 | 0.581 | 3.01 |
| TIP4P/2005 | 278 | 1.001 | 48.02 | 0.062 | 0.700 | 3.75 |
| TIP4P/2005 | 298 | 0.998 | 46.11 | 0.063 | 0.670 | 3.67 |
| TIP4P/2005 | 320 | 0.989 | 45.92 | 0.067 | 0.640 | 3.57 |
| TIP4P/2005 | 340 | 0.979 | 47.32 | 0.073 | 0.616 | 3.48 |

Additional information on the low-$q$ behavior of the structure factor is available from thermodynamics. The limiting value $S(0)$ for $q \to 0$ is connected to the isothermal compressibility $\kappa_T = -1/V(\partial V/\partial P)_T$ by the relation[39]

$$S(0) = \rho k_{\mathrm{B}} T\kappa_T \tag{5}$$

which will be used as a stringent test of the data for $S(q)$ at small but finite $q$.

**Isothermal Compressibility.** The isothermal compressibility is determined by a finite difference method,[41] $\kappa_T = (1/\rho)(\partial\rho/\partial P)_T \approx (\ln(\rho_2/\rho_1))/(P_2 - P_1)$. To evaluate this expression, the system is simulated in a NVT ensemble with the densities $\rho_{1,2} = \rho \pm 0.04$ kg/L, and the resulting pressures $P_{1,2}$ are sampled. Here $\rho$ is the equilibrium density at a pressure of $P$ = 1 bar, as obtained from separate MD simulations (see Table 1). The resulting compressibilities (see Table 1) agree very well with those from previous studies, see e.g. ref 29, where $\kappa_T$ was calculated from volume fluctuations in an isobaric−isothermal ensemble.

**Order Parameters.** To quantify the degree of water structuring, we use two different order parameters. The first one is the tetrahedrality order parameter, $\psi$,[22] with the normalization used by Errington and Debenedetti,[23]

$$\psi = 1 - \frac{3}{8}\sum_{i=1}^{3}\sum_{j=i+1}^{4}\left(\cos(\phi_{ij}) + \frac{1}{3}\right)^2 \tag{6}$$

where $\phi_{ij}$ is the angle formed by the lines connecting the oxygen atom of a given water molecule to the oxygen atoms of its $i$th and $j$th nearest neighbors. Only the four nearest neighbors are taken into account. In order to investigate spatial correlations, we define the spatially resolved tetrahedrality density,

$$\psi(\vec{r}) = \sum_{i=1}^{N}\psi_i\delta(\vec{r} - \vec{r}_i) \tag{7}$$

where $\psi_i$ and $\vec{r}_i$ are the tetrahedrality and the position of the $i$th water molecule.

As a second measure for the water ordering we use the number of hydrogen bonds (HB), $n_{\mathrm{HB}}$, a water molecule forms with its neighbors. Two water molecules are considered to form a HB if the distance between their oxygen atoms is less than $r_{\mathrm{HB}}$ = 0.35 nm and the angle formed by the OH vector of one molecule and the line connecting the oxygen atoms of both molecules is less than $\theta_{HB} = 30°$. Analogously to the tetrahedrality order parameter, we define the spatially resolved HB number density,

$$n_{HB}(\vec{r}) = \sum_{i=1}^{N} n_{HB,i}\delta(\vec{r} - \vec{r}_i) \qquad (8)$$

where $n_{HB,i}$ is the number of HBs the $i$th water molecule forms with its neighbors. Note that, with the above definitions, $\langle n_{HB}(\vec{r})\rangle = \langle n_{HB}\rangle\rho$ and $\langle\psi(\vec{r})\rangle = \langle\psi\rangle\rho$.

## RESULTS

**Structure Factor.** It is a subtle task to extract the low wave vector region of the structure factor $S(q)$ from computer simulations, since the minimal accessible wave vector and the resolution in reciprocal space are restricted by the size of the simulated system. To determine $S(q)$ unambiguously, we use two different methods. The first method, to which we will refer in the following as the Fourier transform (FT) method, makes use of eq 3 to obtain the structure factor from the radial distribution function. The second method (the direct or D method) is to directly calculate $S(q)$ from the simulation trajectories by eq 4. Additionally, we determine the isothermal compressibility $\kappa_T$ to calculate the $q \to 0$ limit of the structure factor, given by $S(0) = \rho k_B T\kappa_T$. The results for the compressibility are summarized in Table 1. We use simulation boxes with a size of roughly 10 × 10 × 10 nm$^3$, containing ≈30 000 water molecules, yielding minimal wave vectors of $q_{min}^{D} \approx 0.6$ nm$^{-1}$ and $q_{min}^{FT} \approx 1.2$ nm$^{-1}$ for the two different methods.

In Figure 1a we show the structure factor of the SPC/E, the TIP4P/2005, and the TIP5P water models at $T = 298$ K and $P = 1$ bar, obtained by the FT method, over a large $q$-range in comparison with experimental results. It can be seen that all water models quite accurately reproduce the position of the first three peaks of the experimental structure factor, while they differ slightly in the height of the peaks, in agreement with earlier simulation results.[37] Figure 1a is mainly shown to stress that the discussion of the low-$q$ region of $S(q)$ for $q < 10$ nm$^{-1}$ concentrates on a small part of the full $S(q)$ curve where the scattering intensity is quite small and relatively featureless.

Figure 1b shows a close-up view of the low-$q$ region of the structure factor for the SPC/E water model at $T = 298$ K, comparing the different methods to extract the structure factor from the simulations. The dashed line marks the result of the FT method, filled circles the results of the direct method, and the $S(q{=}0)$ value obtained from the compressibility is marked by a cross. The solid line is obtained by applying a second-order Savitzky—Golay smoothing filter[44] with a fixed interval width of $\Delta q = 2$ nm$^{-1}$ to the results from the direct method including the $S(q{=}0)$ value obtained from the compressibility. In the FT method results one clearly observes cutoff ripples at low $q$ and pronounced deviations from the direct method results and from the $S(q{=}0)$ value inferred from the compressiblilities. The reason is the high sensitivity of the FT method in the low-$q$ region to statistical fluctuations in the RDF, as we show in the Supporting Information.

Figure 2 shows the low-$q$ region of the structure factor of the SPC/E, the TIP5P, and the TIP4P/2005 water models at different temperatures using the direct method. Also included for comparison are the experimental curves of ref 12 (SAXS). It is seen that, for the TIP5P and TIP4P/2005 water models, there is a pronounced minimum in the structure factor at wave vectors between $q \approx 3$ and 5 nm$^{-1}$, in agreement with previous results for the TIP4P-Ew water model.[16] For the SPC/E model, the minimum is less pronounced but still perceptible. Quantitatively, the results for the SPC/E and TIP5P water models deviate somewhat from the experimental $S(q)$, while the TIP4P/2005 model compares excellently with the experiment. So rather than stressing the differences between different water models, we take as the main message of this figure that all water models studied by us and also the TIP4P-Ew model[16] exhibit an $S(q)$ minimum at small $q$, which means that this is a quite robust feature of classical water models.

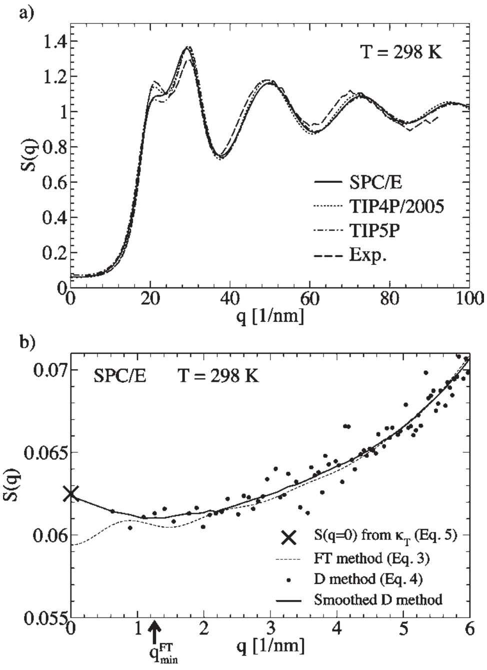

**Figure 1.** (a) Structure factor $S(q)$ obtained by the FT method (see eq 3) at $T = 298$ K and $P = 1$ bar for the SPC/E (full line), TIP4P/2005 (dotted line), and TIP5P (dash-dotted line) water models in comparison with the experimental $S(q)$ (dashed line). The experimental data for the scattering cross-section is taken from a X-ray scattering experiment,[42] and we calculate the structure factor using the isotropic form factor from quantum chemical calculations.[43] (b) Low-$q$ region of the structure factor for SPC/E water at $T = 298$ K and $P = 1$ bar obtained by the FT method (dashed line, see eq 3) and by the direct method (filled circles, see eq 4). The $S(q{=}0)$ value obtained by eq 5 (cross) is also shown. The full line is obtained by smoothing the data from the direct method including the $S(q{=}0)$ value. Note that in the smoothing we did not enforce the slope of $S(q)$ to vanish at $q = 0$.The minimum wave vector of the FT method, $q_{min}^{FT} \approx 1.2$ nm$^{-1}$, is indicated by an arrow.

**Order Parameters.** In the following we investigate to what extent the enhancement seen in the low-$q$ region of the structure factor is related to spatial correlations of the water structure. To that end we examine two structural order parameters and their self- and cross-correlations with the local density. The geometric aspects of the local water ordering can be accurately described by the tetrahedrality order parameter $\psi$, defined in eq 6. For a perfect tetrahedral network $\psi = 1$, while for randomly oriented molecules $\psi = 0$. As a measure for the strength of the hydrogen-bonding network we take the number of hydrogen bonds, $n_{HB}$, a water molecule forms with its neighbors. Here, we adopt the commonly used HOO angle and OO distance criteria for the

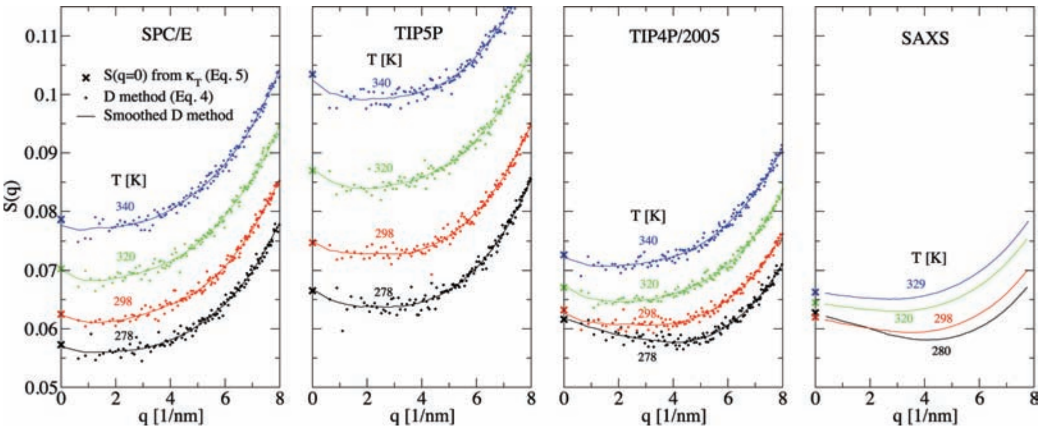

**Figure 2.** Small wave vector region of the structure factor $S(q)$ obtained from MD simulations of the SPC/E, TIP5P, and TIP4P/2005 water models and from experimental SAXS data (taken from ref 12). Filled circles are the result of the direct evaluation of eq 4. The $S(q{=}0)$ values obtained from the compressibility data by eq 5 are marked by crosses. Full lines are obtained by smoothing of the data from the direct method, including the $S(q{=}0)$ values obtained from the compressibility (not enforcing a vanishing slope at the origin). Different colors indicate different temperatures as indicated in the graphs. Experimental compressibilities are taken from ref 3.

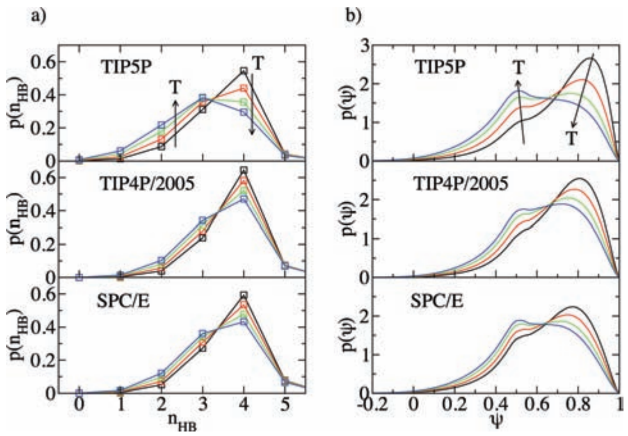

**Figure 3.** (a) Probability distribution $p(n_{\mathrm{HB}})$ of the number of hydrogen bonds, $n_{\mathrm{HB}}$, and (b) probability distribution $p(\psi)$ of the tetrahedrality order parameter, $\psi$, for the TIP5P, TIP4P/2005, and SPC/E water models at temperatures of $T = 278$ (black), 298 (red), 320 (green), and 340 K (blue) and at a pressure of $P = 1$ bar. Arrows indicate the effect of increasing temperature.

hydrogen bond formation.[45] Figures 3 and 4 show the single and joint probability distributions of the two order parameters for the studied water models and varying temperatures. In agreement with previous studies,[23] the tetrahedrality parameter displays a bimodal structure, and for increasing temperature the probability of the high-$\psi$ peak decreases while the probability of the low-$\psi$ peak increases. Similarly, the number of water molecules forming four hydrogen bonds decreases, while the number of water molecules forming three or less hydrogen bonds increases with increasing temperature. From the joint probability distribution (Figure 4), it transpires that the high-$\psi$ peak corresponds to water molecules forming four hydrogen bonds, while the low-$\psi$ peak corresponds to water molecules forming three or less hydrogen bonds. The distinctly different $\psi$ distributions of the subpopulations for $n_{\mathrm{HB}} = 3$ and 4 explains the bimodality of the $\psi$ distributions in Figure 3.

**Correlation Functions.** To gain information about spatial correlations of the different local water configurations, we define

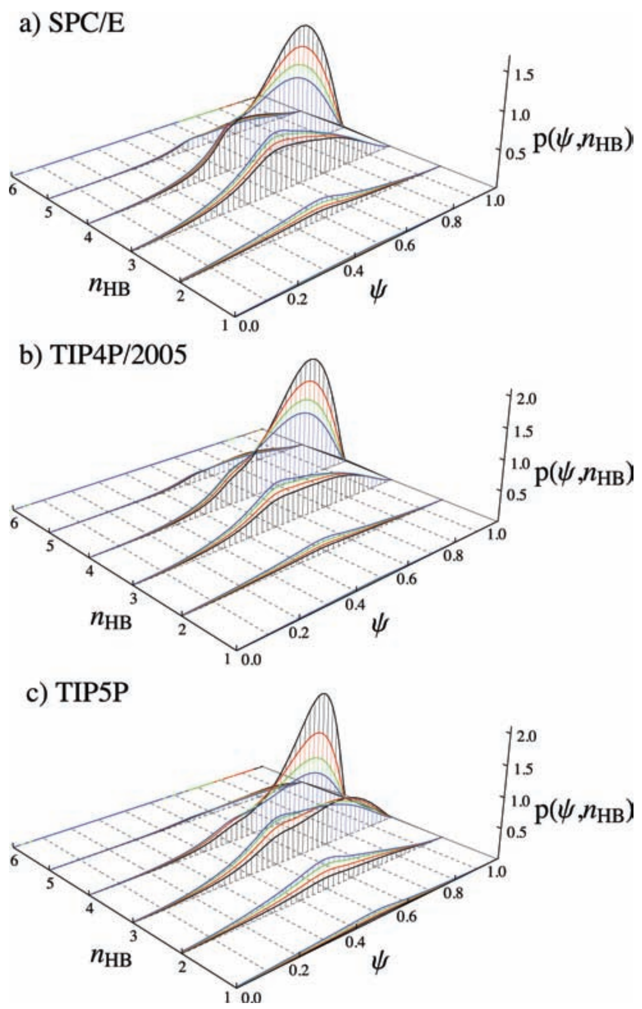

**Figure 4.** Joint probability distribution $p(\psi, n_{\mathrm{HB}})$ of the number of hydrogen bonds, $n_{\mathrm{HB}}$, and the tetrahedrality order parameter, $\psi$, for the (a) SPC/E, (b) TIP4P/2005, and (c) TIP5P water models at temperatures of $T = 278$ (black), 298 (red), 320 (green), and 340 K (blue) and at a pressure of $P = 1$ bar.

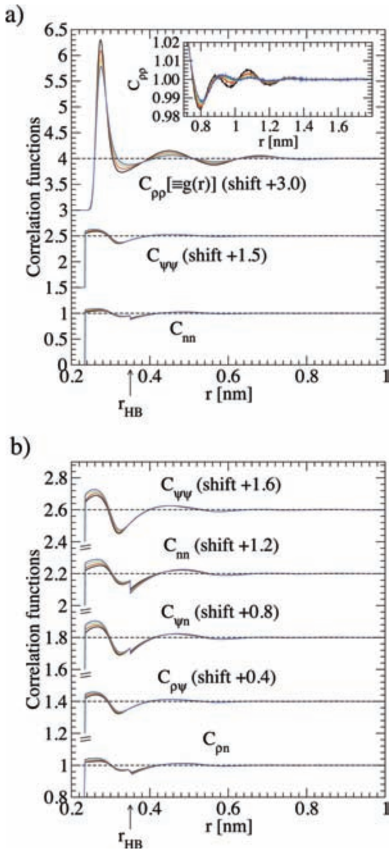

**Figure 5.** (a) Self-correlation functions of density, $C_{\rho\rho}$, tetrahedrality order parameter, $C_{\psi\psi}$, and the number of hydrogen bonds, $C_{nn}$. The inset shows an enlarged view of the long-range region of the density self-correlation function. (b) Comparison of the self- and cross-correlation functions of the density and the structural order parameters. For clarity some curves are shifted as indicated in the figure. All data are obtained by MD simulations of the SPC/E water model at temperatures of $T = 278$ (black), 298 (red), 320 (green), and 340 K (blue) and at a pressure of $P = 1$ bar.

two-point correlation functions of the various local order parameters. In Figure 5a we show the normalized self-correlation function for the density,

$$C_{\rho\rho}(r) = g(r) = \frac{\langle \rho(0)\rho(r)\rangle}{\rho^2} \tag{9}$$

and the normalized self-correlation functions,

$$C_{\psi\psi}(r) = \frac{\langle \psi(0)\psi(r)\rangle}{\langle \psi\rangle^2 \langle \rho(0)\rho(r)\rangle} \tag{10}$$

and

$$C_{nn}(r) = \frac{\langle n_{\mathrm{HB}}(0)n_{\mathrm{HB}}(r)\rangle}{\langle n_{\mathrm{HB}}\rangle^2 \langle \rho(0)\rho(r)\rangle} \tag{11}$$

of the tetrahedrality order parameter and the hydrogen bond numbers for the SPC/E water model at temperatures of $T = 278, 298, 320,$ and 340 K. All correlation functions are normalized to unity at large separations. In addition, we normalize the functions $C_{\psi\psi}(r)$ and $C_{nn}(r)$ by the density density correlation function $C_{\rho\rho}(r)$ such that, in the absence of variations in the tetrahedrality parameter $\psi$ or hydrogen bond number $n_{\mathrm{HB}}$, the functions would be constant. In contrast to the density density correlation function $C_{\rho\rho}(r)$, the self-correlation functions $C_{\psi\psi}(r)$ and $C_{nn}(r)$ are quite featureless and thus show that there are only weak correlations between structural fluctuations. The weak correlations that one can discern decay to zero after ≈6 Å. Note that the small jump seen in the correlation function $C_{nn}$ (indicated by a vertical arrow) is due to the HB cutoff radius $r_{\mathrm{HB}} = 0.35$ nm of the hydrogen bond criterion.

In Figure 5b the self-correlation functions $C_{\psi\psi}(r)$ and $C_{nn}(r)$ are compared with the cross-correlation functions,

$$C_{\psi n}(r) = \frac{\langle \psi(0)n_{\mathrm{HB}}(r)\rangle}{\langle \psi\rangle\langle n_{\mathrm{HB}}\rangle\langle \rho(0)\rho(r)\rangle} \tag{12}$$

$$C_{\rho\psi}(r) = \frac{\langle \rho(0)\psi(r)\rangle}{\langle \psi\rangle\langle \rho(0)\rho(r)\rangle} \tag{13}$$

and

$$C_{\rho n}(r) = \frac{\langle \rho(0)n_{\mathrm{HB}}(r)\rangle}{\langle n_{\mathrm{HB}}\rangle\langle \rho(0)\rho(r)\rangle} \tag{14}$$

Not surprisingly, the self- and cross-correlation functions of the tetrahedrality parameter and the hydrogen bond number show similar behavior, in line with the results from Figure 4, which point to a close correspondence between the two order parameters. We see that there are only weak spatial correlations between these two measures of the local water structure; in other words, the degree to which a given water molecule is tetrahedrally ordered or hydrogen-bonded is only very weakly correlated to the structural ordering of a neighboring water molecule. Note that Figure 4 tells us that the structural distribution functions are quite broad, so we learn that, while structural fluctuations are pronounced, their spatial correlation is weak. Interestingly, the cross-correlation functions $C_{\rho\psi}$ and $C_{\rho n}$ between the density and the two structural order parameters exhibit even weaker correlations than the other correlation functions. In disagreement with the arguments brought forward in ref 12, we see that there is very little correlation between density and structural fluctuations, meaning specifically that features in $S(q)$ data unfortunately tell us very little about the spatial correlations of water structure. In the Supporting Information (see Figure S2) we show the normalized self- and cross-correlation functions of the density and the structural order parameters for the SPC/E, the TIP4P/2005, and the TIP5P water models for different temperatures. The qualitative behavior does not differ much between the different water models. In agreement with previous findings,[40] the TIP5P water model is slightly overstructured in comparison with the TIP4P/2005 and SPC/E water models.

## ■ CONCLUSION AND DISCUSSION

We show that, for several commonly used water models at temperatures above melting, there exist only weak spatial correlations between different structural order parameters. The typical range of structural correlations in Figure 5 is consistent with a decay length on the order of 1 Å, as observed in ref 18 for a coarse-grained water model. The relation of such a decay length with a correlation length as inferred from an Ornstein−Zernike analysis of the structure factor is, however, far from clear.[16] We furthermore do not observe a pronounced spatial correlation between structural and density fluctuations, implying that features in the structure factor cannot be interpreted in terms of or associated with structural properties, in contradiction to the assumptions made in ref 12 and in line with the results in ref 16. Errington et al.[17] report a reciprocal coupling between the tetrahedrality and the density in tetrahedrally ordered clusters in SPC/E water at low temperatures of $T = 220$ and 240 K. That we find very weak spatial coupling between the density and the tetrahedral ordering in two-point correlation functions suggests that the clustering result of Errington et al.[17] involves multipoint correlations. At this point it is important to stress that the correlations we find between local density and structure are not totally absent, but they are rather much smaller than the density—density correlations (see Figure 5). So whether one calls the density—structure correlation small or large depends on which reference one is using for comparison. Our results are consistent with the findings of Matsumoto,[19] who observed no direct relation between the density anomaly and structural heterogeneities but rather an interplay of monotonic hydrogen bond extension and angular distortion in the network (see Figure 3) upon cooling. While the spatially averaged values of the density and the hydrogen-bonding network distortion are, of course, related, we show that their fluctuations are not strongly correlated in space. The picture of coexisting domains of differently structured water is not supported by an analysis of the respective two-point correlation functions. Such correlations might grow as temperature is lowered into the metastable liquid regime below melting and one approaches the liquid—liquid critical point, which however is not the focus of the present paper.

We also show that the experimentally well documented minimum in the structure factor at small wave vector $q$, which has very recently been seen in simulations of TIP4P-Ew water,[16] is obtained with different simple water models, suggesting that this is a quite robust feature, which in fact is related to the interplay of attractive and repulsive forces.[21,46] Finally, let us stress that we are not claiming that classical water models can accurately describe all aspects of water structure; however, the low-$q$ behavior of $S(q)$ does not constitute a serious hurdle for current classical water models.

## ■ ASSOCIATED CONTENT

Ⓢ **Supporting Information.** Simulation details, discussion of the cutoff dependence of the structure factor via the FT method, correlation functions for the SPC/E, TIP4P/2005, and TIP5P water models, and complete ref 12. This material is available free of charge via the Internet at http://pubs.acs.org.

## ■ AUTHOR INFORMATION

### Corresponding Author

netz@ph.tum.de

## ■ ACKNOWLEDGMENT

Financial support by the Elitenetzwerk Bayern in the framework of the doctorate program Materials Science of Complex Interfaces and the Deutsche Forschungsgemeinschaft (DFG Grant NE 810/7), and the Ministry for Economy and Technology (BMWi) in the framework of the AiF project “Simulation and prediction of salt influence on biological systems” is gratefully acknowledged. The authors thank the Leibniz-Rechenzentrum München (LRZ) for computing time on HLRB-II (Project pr28xe).

## ■ REFERENCES

(1) Franks, F. *Water. A Comprehensive Treatise*; Plenum: New York, 1973.

(2) Angell, C.; Shuppert, J.; Tucker, J. *J. Phys. Chem.* **1973,** *77*, 3092–3099.

(3) Kell, G. S. *J. Chem. Eng. Data* **1975,** *20*, 97–105.

(4) Saul, A.; Wagner, W. *J. Phys. Chem. Ref. Data* **1989,** *18*, 1537–1564.

(5) Speedy, R.; Angell, C. *J. Chem. Phys.* **1976,** *65*, 851–858.

(6) Poole, P.; Sciortino, F.; Essmann, U.; Stanley, H. *Nature* **1992,** *360*, 324–328.

(7) Speedy, R. *J. Phys. Chem.* **1982,** *86*, 982–991.

(8) Stanley, H. E.; Teixeira, J. *J. Chem. Phys.* **1980,** *73*, 3404–3422.

(9) Debenedetti, P. G. *J. Phys.: Condens. Matter* **2003,** *15*, 1669–1726.

(10) Mishima, O.; Stanley, H. E. *Nature* **1998,** *396*, 329–335.

(11) Sastry, S.; Debenedetti, P. G.; Sciortino, F.; Stanley, H. E. *Phys. Rev. E* **1996,** *53*, 6144–6154.

(12) Huang, C.; et al. *Proc. Natl. Acad. Sci. U.S.A.* **2009,** *106*, 15214–15218.

(13) Bosio, L.; Teixeira, J.; Stanley, H. E. *Phys. Rev. Lett.* **1981,** *46*, 597–600.

(14) Bosio, L.; Teixeira, J.; Bellissent-Funel, M.-C. *Phys. Rev. A* **1989,** *39*, 6612–6613.

(15) Xie, Y.; Jr, K. F. L.; Morales, G.; Hare, D. E.; Sorensen, C. M. *Phys. Rev. Lett.* **1993,** *71*, 2050–2053.

(16) Clark, G.; Hura, G.; Teixeira, J.; Soper, A.; Head-Gordon, T. *Proc. Natl. Acad. Sci. U.S.A.* **2010,** *107*, 14003–14007.

(17) Errington, J. R.; Debenedetti, P. G.; Torquato, S. *Phys. Rev. Lett.* **2002,** *89*, 215503.

(18) Moore, E. B.; Molinero, V. *J. Chem. Phys.* **2009,** *130*, 244505.

(19) Matsumoto, M. *Phys. Rev. Lett.* **2009,** *103*, No. 017801.

(20) Molinero, V.; Moore, E. *J. Phys. Chem. B* **2009,** *113*, 4008–4016.

(21) Soper, A. K.; Teixeira, J.; Head-Gordon, T. *Proc. Natl. Acad. Sci. U.S.A.* **2010,** *107*, No. E44—E44.

(22) Chau, P.; Hardwick, A. *Mol. Phys.* **1998,** *93*, 511–518.

(23) Errington, J. R.; Debenedetti, P. G. *Nature* **2001,** *409*, 318–321.

(24) Kumar, P.; Buldyrev, S.; Stanley, H. *Proc. Natl. Acad. Sci. U.S.A.* **2009,** *106*, 22130.

(25) Berendsen, H. J. C.; Grigera, J. R.; Straatsma, T. P. *J. Phys. Chem.* **1987,** *91*, 6269–6271.

(26) Abascal, J.; Vega, C. *J. Chem. Phys.* **2005,** *123*, 234505.

(27) Mahoney, M.; Jorgensen, W. L. *J. Chem. Phys.* **2000,** *112*, 8910.

(28) Baez, L.; Clancy, P. *J. Chem. Phys.* **1994,** *101*, 9837–9840.

(29) Pi, H. L.; Aragones, J. L.; Vega, C.; Noya, E. G.; Abascal, J. L. F.; Gonzalez, M. A.; McBride, C. *Mol. Phys.* **2009,** *107*, 365–374.

(30) Giovambattista, N.; Stanley, H. E.; Sciortino, F. *Phys. Rev. E* **2005,** *72*, No. 031510.

(31) Brovchenko, I.; Geiger, A.; Oleinikova, A. *J. Chem. Phys.* **2005,** *123*, No. 044515.

(32) Harrington, S.; Poole, P. H.; Sciortino, F.; Stanley, H. E. *J. Chem. Phys.* **1997,** *107*, 7443–7450.

(33) Essmann, U.; Perera, L.; Berkowitz, M. L.; Darden, T.; Lee, H.; Pedersen, L. *J. Chem. Phys.* **1995,** *103*, 8577–8593.

(34) Darden, T.; York, D.; Pedersen, L. *J. Chem. Phys.* **1993,** *98*, 10089–10092.

(35) Lsal, M.; Kolafa, J.; Nezbeda, I. *J. Chem. Phys.* **2002,** *117*, 8892–8897.

(36) Xu, L.; Kumar, P.; Buldyrev, S. V.; Chen, S.; Poole, P. H.; Sciortino, F.; Stanley, H. E. *Proc. Natl. Acad. Sci. U.S.A.* **2005,** *102*, 16558–16562.

(37) Jorgensen, W. L.; Chandrasekhar, J.; Madura, J. D.; Impey, R.; Klein, M. L. *J. Chem. Phys.* **1983,** *79*, 926–935.

(38) Waser, J.; Schomaker, V. *Rev. Mod. Phys.* **1953,** *25*, 671–690.

(39) Hansen, J. P.; McDonald, I. R. *Theory of simple liquids*, 3rd ed.; Academic Press: Amsterdam, 2006.

(40) Sorenson, J. M.; Hura, G.; Glaeser, R. M.; Head-Gordon, T. *J. Chem. Phys.* **2000,** *113*, 9149–9161.

(41) Motakabbir, K. A.; Berkowitz, M. L. *J. Phys. Chem.* **1990,** *94*, 8359–8362.

(42) Hura, G.; Sorenson, J. M.; Glaeser, R. M.; Head-Gordon, T. *J. Chem. Phys.* **2000,** *113*, 9140–9148.

(43) Wang, J.; Tripathi, A. N.; Smith, V. H. *J. Chem. Phys.* **1994,** *101*, 4842–4854.

(44) Savitzky, A.; Golay, M. *Anal. Chem.* **1964,** *36*, 1627–1639.

(45) Kumar, R.; Schmidt, J. R.; Skinner, J. L. *J. Chem. Phys.* **2007,** *126*, 204107.

(46) Weeks, J. D.; Chandler, D.; Andersen, H. *J. Chem. Phys.* **1971,** *54*, 5237–5247.